

See discussions, stats, and author profiles for this publication at: <https://www.researchgate.net/publication/30413706>

A small-angle neutron scattering study of a semi-flexible main-chain liquid-crystalline copolyester. *Macromolecules*

ARTICLE *in* MACROMOLECULES · SEPTEMBER 1992

Impact Factor: 5.8 · DOI: 10.1021/ma00046a030 · Source: OAI

CITATIONS

36

READS

10

4 AUTHORS, INCLUDING:



[Valeria Arrighi](#)

Heriot-Watt University

90 PUBLICATIONS 1,097 CITATIONS

SEE PROFILE



[R. A. Weiss](#)

University of Akron

227 PUBLICATIONS 5,223 CITATIONS

SEE PROFILE

A Small-Angle Neutron Scattering Study of a Semiflexible Main-Chain Liquid Crystalline Copolyester

V. Arrighi and J. S. Higgins*

Chemical Engineering Department, Imperial College, London SW7 2BY, U.K.

R. A. Weiss and A. L. Cimecioglu

Institute of Materials Science, University of Connecticut, Storrs, Connecticut 06269-3136

Received February 18, 1992; Revised Manuscript Received June 22, 1992

ABSTRACT: A main-chain semiflexible copolyester containing 4,4'-dihydroxy- α,α' -dimethylbenzalazine as the mesogenic unit has been studied by small-angle neutron scattering (SANS). The polyester shows a nematic phase in the temperature range between 160 and 250 °C. The polymer chain conformation, in the nematic phase range, was investigated for mixtures of deuterated and hydrogenous polymers, aligned using a magnetic field ($B_0 = 0.6$ T). Due to the occurrence of a transesterification reaction, polymer chains consisting of deuterated and nondeuterated blocks of different lengths are formed, as a function of annealing time. The average degree of polymerization and the radius of gyration of the blocks were measured from the neutron scattering profiles. Changes in chain anisotropy have been observed in the nematic phase range, as predicted by recent theories developed for semiflexible main-chain liquid crystalline polymers (LCPs). A persistence length of 120 Å was measured in the temperature range from 175 to 196 °C for a mixture consisting of fully deuterated LCP and unlabeled polymer. The scattering from the pure polymers aligned in the mesophase was also investigated. The results suggest that the disclination structure associated with a domain structure, typical of liquid crystalline systems, may be observable by SANS.

Introduction

The liquid crystalline behavior in monomeric liquid crystals is generally associated with a rigid asymmetric molecular shape.¹ This gives rise to anisotropic intermolecular interactions responsible for the occurrence of liquid crystallinity. In analogy, polymers giving rise to highly extended structures would be expected to exhibit similar liquid crystalline properties. However, when the mesogenic units are directly connected to each other, the resulting linear rigid-rod macromolecule has a high melting temperature.² Decomposition usually occurs before the compound shows any thermotropic liquid crystalline behavior. At the same time, the formation of a lyotropic liquid crystalline phase may also be prevented by the poor solubility of the rigid structures.

The introduction of flexible spacers (alkylene or alkoxy chains) between the rigid aromatic units in the polymer main chain is a proven method for obtaining liquid crystalline polymer melts. The resulting polymers are termed main-chain, semiflexible liquid crystalline polymers (LCPs).^{3,4} The reduction of the melting temperature to values at which the melt is processable in the liquid crystalline state leads to improved mechanical properties, suitable for important technological applications such as high modulus fibers and self-reinforcing polymer blends.⁵

The characterization of the polymer chain conformation is of significant importance in the understanding of their macroscopic properties, i.e., their mechanical properties. In particular, a fully extended conformation is expected to have outstanding mechanical properties.

A number of theoretical approaches have been developed in order to model the first-order transition in LCPs. Although early theories developed by Onsager⁶ and Flory⁷ were essentially devoted to lyotropic LCPs composed of rigid macromolecules, recently theoretical treatments have appeared in the literature which apply to semiflexible LCPs.⁸⁻¹⁰ In these polymeric systems, the competition between the long-range orientational order, typical of a

nematic phase, and the tendency of the polymer to maximize its entropy by assuming a random-coil conformation is expected to give rise to important conformational changes at the isotropic to nematic transition. As pointed out by de Gennes,¹¹ the semiflexible chain may recover some part of the entropy loss due to the ordering of the mesogenic units either by undulating about the ordering direction or by forming hairpin defects due to the abrupt changes in chain direction.

An analysis of the chain statistics in a nematic field has been performed by Warner et al.^{8,12} The semiflexible chains are described as a continuous elastic bending curve, adopting a wormlike chain model. The model is applied to liquid crystalline phases with the addition of the interaction potential between chains. A mean-field potential of the Maier and Saupe type has been considered by Warner et al.⁸ and ten Bosch et al.^{9,10} The anisotropy of the chain conformation of a main-chain LCP in a nematic phase has been predicted to increase exponentially with decreasing temperature, due to the disappearance of hairpins.^{8,12}

Small-angle neutron scattering (SANS) has been successfully applied to the study of the polymer conformation in the bulk state.¹³ The technique has been recently extended to investigate the polymer chain conformation in an anisotropic environment for side-chain LCPs.¹⁴⁻¹⁷ Only a few measurements of polymer chain conformation of main-chain semiflexible LCPs have been reported. Measurements were conducted by D'Allest et al.^{18,19} on semiflexible LCPs aligned in a magnetic field (1.4 T). The polymer investigated was a polyester containing *p,p'*-dioxy-2,2'-dimethylazoxybenzene as the mesogen and a flexible spacer consisting of either 10 (DDA-9) or 7 (AZA-9) methylene units. An increase in chain dimensions was observed at the isotropic to nematic phase transition. Values of the radius of gyration (R_g) in the isotropic liquid phase were comparable to those obtained from unaligned samples and indicative of a random-coil conformation. In the nematic phase, the R_g values reported for DDA-9 indicated a high degree of chain extension which approached an almost

* To whom correspondence should be addressed.

Chart I

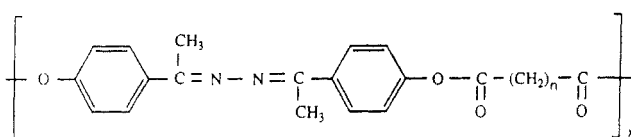


Table I
Designation and Characteristics of the Polymers

polymer	η_{inh}^d (dL g ⁻¹)	M_w (GPC) ^e	M_w/M_n	M_w (LS) ^f
H11 ^a	0.59	43 600	2.4	12 500
H16 ^a	0.61	38 100	2.4	14 500
D2 ^b	0.44			8 600
D6 ^c	0.67			16 300

^a Hydrogenous polymers. ^b Partially labeled polymer, deuterated in the flexible spacers with $n = 8$ and 10 methylene units. ^c Fully deuterated LCP. ^d Measured at concentration 0.5 g/dL in CHCl₃ at 25 °C. ^e From gel permeation chromatography (GPC) expressed as "polystyrene equivalent". ^f Calculated from eq 1.

fully extended conformation. That finding was probably due to the fact that their LCPs were of relatively low molecular weight (i.e., 4000–5000).

We present a study of chain conformation in the nematic phase of a copolyester of 4,4'-dihydroxy- α,α' -dimethylbenzalazine (DMB; Chart I) with a 50/50 composition of 8 and 10 methylene group spacers. The thermotropic behavior of polyesters of DMB was first recognized by Roviello and Sirigu.³ They reported the synthesis of various copolyesters with a wide range of mesophase stability.²⁰ The copolymer used in the present study exhibits nematic thermotropic behavior over a wide temperature range (approximately 100 °C). It is thus suitable for investigations of the temperature dependence of chain extension within the mesophase range.

It is well-known that in polymers of the condensation type such as polyesters interchange reactions may occur during heating above the melting temperature. In this study, the occurrence of transesterification between the labeled and unlabeled polymer chains was observed by SANS during annealing of the samples. It is shown in this study that, although transesterification may interfere with measurements of chain conformation, it is still possible to extract information on chain anisotropy and chain rigidity.

Experimental Section

Sample Characterization. The hydrogenous and deuterated polymers were synthesized as described in ref 21. A polymer deuterated only in the two flexible spacers (D2) and one deuterated both in the flexible chains and the rigid mesogenic unit (D6) were used during the SANS experiments together with two hydrogenous polymers (H11 and H16) of different molecular weights. The molecular weights and molecular weight distributions were determined by gel permeation chromatography (GPC). The characteristics of the polymers employed in SANS measurements are listed in Table I. Values of η_{inh} indicate the inherent viscosity measured in chloroform solutions at a polymer concentration equal to 0.5 g/dL and $T = 25$ °C. The molecular weights indicated as M_w (LS) in Table I refer to values calculated from the intrinsic viscosity, $[\eta]$, using the relationship

$$[\eta] = 9.6 \times 10^{-4} M_w^{0.68} \quad (1)$$

which was derived from measurements of M_w by means of light scattering and viscosity measurements as described in ref 21. It is clear from data reported in Table I that there is a large difference between molecular weights determined by GPC and values calculated from $[\eta]$ using eq 1. Since M_w (GPC) have been expressed as "polystyrene equivalent", the difference in hydrodynamic volume of polyesters of DMB and polystyrene is probably responsible for the high M_w values measured by GPC. On the other hand, M_w (LS) give absolute values of molecular weights.

Table II
Transition Temperatures and Enthalpy and Entropy Changes for Pure Copolymers

polymer	run ^a	T_m' (°C)	T_m (°C)	T_{NI} (°C)	ΔH_m (kcal mol ⁻¹)	ΔH_{NI} (kcal mol ⁻¹)	ΔS_{NI} (cal mol ⁻¹ K ⁻¹)
H11	h1		162	250	1.77	2.21	4.22
	c1		129	236	-2.21	-1.98	-4.05
	h2	142	150	241	2.00	2.11	4.12
H16	h1		162	250	1.42	2.15	4.22
	c1		107	229	-1.35	-1.92	-3.82
D2	h2	117	137	245	0.92	2.11	4.07
	h1		151	236	1.93	1.85	3.63
D6	c1		101	209	-1.41	-1.24	-2.57
	h2	116	134	217	2.16	1.71	3.49
	h1		162	251	1.45	2.22	4.24

^a h1 = first heating run (heating rate, 20 °C/min), c1 = first cooling run (cooling rate, 10 °C/min), h2 = second heating run (heating rate, 20 °C/min).

The thermal behavior of copolyesters of dimethylbenzalazine was investigated by differential scanning calorimetry (DSC) using either a DSC-2 or DSC-7 Perkin-Elmer differential scanning calorimeter. Measurements were conducted using thermally untreated samples. First heating (heating rate, 20 °C/min), first cooling (cooling rate, 10 °C/min), and second heating (20 °C/min) curves were recorded for all samples. The polymer shows a glass transition temperature at 25 °C. Transition temperatures from the solid to the nematic phase (T_m) and from the nematic to the isotropic liquid phase (T_{NI}) are listed in Table II. Molar melting enthalpy (ΔH_m), molar isotropization enthalpy (ΔH_{NI}), and entropy (ΔS_{NI}) are also listed in Table II.

Sample Preparation. SANS samples consisted of mixtures containing the hydrogenous and deuterated polymers (either partially or fully deuterated) in approximately the same weight percentage. This composition achieved maximum scattered intensity. The polymer mixtures were prepared by dissolving the labeled and unlabeled copolyesters in chloroform. After filtering the solution, the solvent was removed by evaporation and the mixture was dried in vacuo.

Samples were prepared by molding the powder into a sample holder at temperatures above the melting point (typically $T \sim 200$ °C). Films having thicknesses from 1.2 to 1.7 mm and a diameter equal to 12 mm were produced.

Pure copolymer samples (fully deuterated, partially deuterated, and hydrogenous) were also prepared by SANS measurements.

Small-Angle Neutron Scattering. SANS measurements were carried out on the D11 diffractometer at the Institut Laue-Langevin (Grenoble, France).²² A sample-to-detector distance of 10 m and a wavelength of 8 Å were used during all experiments, giving a range of scattering vectors from 0.004 to 0.025 Å⁻¹. The wavelength resolution $\Delta\lambda/\lambda$ was equal to 45% which allowed a higher neutron flux to be obtained. This reduced the long counting times required for the analysis of scattering of anisotropic patterns and enabled us to study the chain anisotropy as a function of time.

Measurements of chain conformation were performed by aligning the sample in a magnetic field at temperatures within the nematic phase. The samples were heated in a brass cell placed within the poles of an electromagnet (Magnet B-E 10), producing a field in the direction perpendicular to the incident neutron beam. The strength of the magnetic field was from 0.6 to 0.7 T. Temperature was controlled within ± 1 °C.

The scattering from the following samples was measured: (a) deuterated-hydrogenous LCP mixtures, (b) pure polymers (fully deuterated, partially deuterated, hydrogenous), (c) sample holder, (d) water sample (thickness = 1 mm), and (e) the water cell.

Some measurements were also performed on the LOQ small-angle diffractometer²³ at the Rutherford Appleton Laboratory (Oxon, U.K.). In this case, the explored Q range was from 0.006 to 0.22 Å⁻¹.

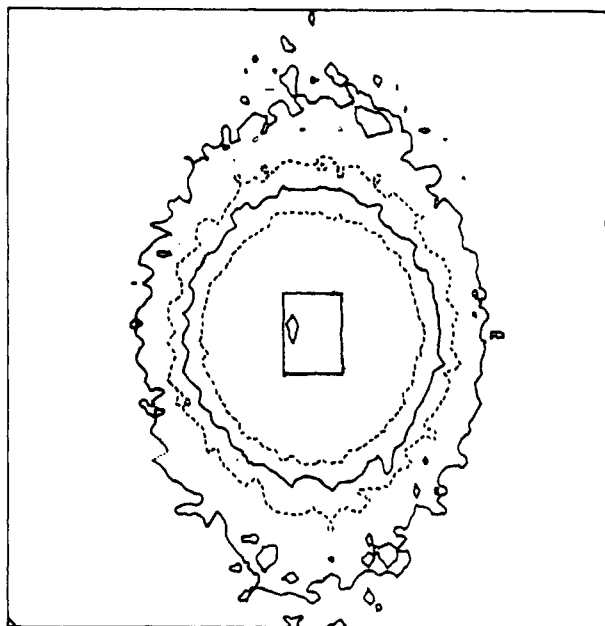


Figure 1. Contour intensity plot (raw data) from a 45% fully deuterated LCP mixture (45D6-H16) aligned at 175 °C, under magnetic field (horizontal direction in the picture) for 20 min.

Data Analysis. Data analysis was performed according to ILL-supported routines.²⁴ For isotropic scattering, the two-dimensional data (neutron counts in each cell of the detector) were circularly averaged to derive the radial distribution of the scattered intensity $I(r)$ (r being the distance from the center of the detector). This was converted to $I(Q)$, the scattering intensity as a function of the scattering vector, using the relationship

$$Q = \frac{4\pi}{\lambda} \sin \frac{\theta}{2} = \frac{2\pi}{\lambda} \frac{r}{d_{S-D}} \quad (2)$$

where θ is the scattering angle, λ the wavelength, and d_{S-D} the sample-to-detector distance. Corrections included subtraction of the scattering from the sample holder, normalization to the same number of monitor counts, and correction for sample transmission and thickness. The total (coherent and incoherent) differential scattering cross section in units cm^{-1} was determined using water as a calibration standard.

A different procedure was adopted for anisotropic scattering. Data were first normalized to absolute units. Averaging was then performed in 30° sectors, centered around the directions parallel and perpendicular to the direction of the applied magnetic field.

The coherent differential scattering cross section ($d\Sigma(Q)/d\Omega$) was obtained by subtracting the incoherent scattering from isotropic and anisotropic patterns. The incoherent scattering was estimated from the scattering of pure hydrogenous and deuterated samples.

The use of the 45% velocity selector introduces a higher degree of uncertainty in the results compared to measurements obtained with the usual 9% velocity selector. The effect of a large wavelength distribution on data analysis has already been discussed in the literature.²⁵ It is possible to demonstrate that an apparent radius of gyration, R_g , is determined in this case which is approximately 5% larger than the true R_g . No correction factors were applied to the results reported in this work.

Results and Discussion

A contour plot of the scattered intensity in the plane normal to the incident beam direction is shown in Figure 1 for a sample consisting of a mixture of fully deuterated (45% by weight) and hydrogenous polymer (indicated as 45D6-H16) aligned in a magnetic field at 175 °C for 20 min. All mixtures of labeled and unlabeled LCP aligned in the nematic phase range exhibited similar anisotropic scattering patterns. The scattering patterns were elongated in the direction perpendicular to the applied field,

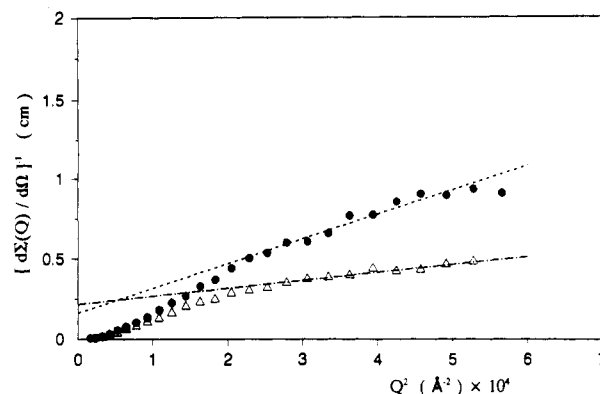


Figure 2. Coherent scattered intensity, plotted according to the Zimm equation, for 45D6-H16 aligned at 175 °C: (●) direction parallel and (Δ) perpendicular to the applied magnetic field (lines represent least-squares fits).

indicating that the polymer chains were aligned in the direction parallel to the field. Isotropic contour plots were obtained for the pure polymers aligned in the LC phase and for polymer mixtures containing the labeled LCP (D2 or D6) subjected to a magnetic field in the isotropic liquid phase ($T > 250$ °C).

The weight-average molecular weight, M_w , and the z -average radius of gyration, $\langle R^2 \rangle_z^{1/2}$, of the deuterated chains in a hydrogenous matrix can be determined by the analysis of the measured differential scattering cross section, $d\Sigma(Q)/d\Omega$, in the Guinier range ($QR_g < 1$), according to the Zimm equation.¹³ A similar treatment can be applied to analyze anisotropic scattering patterns. In the limit of small angles, the coherent differential scattering cross section can be expressed as a function of the projections of the radius of gyration in the direction parallel and perpendicular to the direction of alignment, according to

$$\left[\frac{d\Sigma(Q_{\parallel})}{d\Omega} \right]^{-1} = \left[\frac{d\Sigma(0)}{d\Omega} \right]^{-1} [1 + Q_{\parallel}^2 R_{\parallel}^2]$$

$$\left[\frac{d\Sigma(Q_{\perp})}{d\Omega} \right]^{-1} = \left[\frac{d\Sigma(0)}{d\Omega} \right]^{-1} [1 + Q_{\perp}^2 R_{\perp}^2] \quad (3)$$

where Q_{\parallel} and Q_{\perp} indicate the components of the scattering vector in the directions parallel and perpendicular to the applied field and R_{\parallel} and R_{\perp} are the z -average mean-square displacement of the radius of gyration, $\langle R^2 \rangle_z^{1/2}$, in the two directions. Equation 3 is valid in the Guinier range when $Q_{\parallel} R_{\parallel} < 1$ and $Q_{\perp} R_{\perp} < 1$. The intercept at $Q = 0$ in eq 3 is related to the weight-average molecular weight, M_w , through the relationship

$$\frac{d\Sigma(0)}{d\Omega} = M_w x (1-x) \rho N_A (b_D - b_H)^2 / M_0^2 \quad (4)$$

where x represents the mole fraction of deuterated chains in the polymer mixture, ρ is the polymer density, N_A is Avogadro's number, b_D and b_H are the scattering length of the labeled and unlabeled monomers, respectively, and M_0 is the molecular weight of the polymer repeat unit. This type of analysis has been applied to the study of the chain anisotropy in both side-chain and main-chain LCPs macroscopically aligned by magnetic fields.^{18,19}

Zimm plots of the measured scattered intensity parallel and perpendicular to the magnetic field for a 45% fully deuterated LCP mixture aligned at 175 °C are shown in Figure 2. Deviations from linear behavior occurred, at low scattering vectors, which may be attributed to either the presence of voids, partial segregation between the

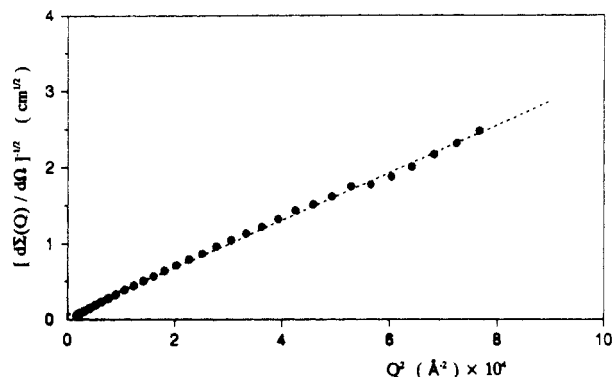


Figure 3. Debye-Bueche plot for fully deuterated LCP (D6) aligned at 191 °C in a magnetic field: (●) data points and (---) least-squares fit.

hydrogenous and deuterated polymers in the sample mixture, or the mesophase microstructure.

SANS of Pure Polymers. In order to analyze in detail the scattering patterns and particularly the behavior at low scattering vectors, SANS measurements were made on a fully deuterated (D6), partially deuterated (D2), and hydrogenous (H16) LCP samples. The experiments were performed by aligning the samples in a magnetic field at an intermediate temperature within the mesophase range ($T = 191$ °C). After subtraction of the incoherent scattering, a coherent signal was present in the scattering curve of the pure polymers. The intensity was higher for the fully deuterated LCP, which was due to its higher cross section with respect to the partially labeled and unlabeled LCPs. These results suggest that the labeled and unlabeled LCP in the polymer mixture give rise to a similar coherent scattering as observed in the pure polymers. This signal, superimposed on the single-chain scattering (described by eq 3), was assumed to be responsible for the deviations from linearity observed in the Zimm plots (Figure 2). This excludes segregation between the hydrogenous and deuterated chains in the labeled-unlabeled mixtures.

Data from the fully deuterated LCP aligned at 191 °C were analyzed according to the Debye-Bueche model.²⁶ This describes fluctuations in scattering length density (defined as the scattering length per unit molecular volume) within a two-phase system where the two phases are randomly distributed and have irregular shape and size. Analysis of the scattering curve allows a correlation length, a_c , to be determined according to the relationship

$$\frac{d\Sigma(Q)}{d\Omega} = \frac{K\langle\rho_b^2\rangle a_c^3}{(1 + Q^2 a_c^2)^2} \quad (5)$$

where $\langle\rho_b^2\rangle$ represents the mean-square fluctuation in scattering length density and K is a constant. A plot of the inverse square root of the measured intensity versus Q^2 is shown in Figure 3 for D6 aligned at 191 °C. The correlation length, calculated from the slope to intercept ratio, is equal to 225 ± 30 Å. Similar values were measured from a Debye-Bueche analysis of the scattering curves for the partially deuterated (D2) and fully hydrogenous (H16) LCP, at the same temperature. However, the intensity of the signal differed substantially for the three polymers; it appeared to be approximately proportional to the respective scattering length densities.

The temperature and time dependences of the scattering from the fully deuterated LCP were also investigated. The correlation length was found to slowly increase with annealing time. At $T = 191$ °C, a change of a_c from 208 ± 18 to 258 ± 28 Å was observed after 1 h of annealing.

Table III
Correlation Length for Fully Deuterated LCP (D6):
Temperature Dependence

T (°C)	a_c (Å)	$K\langle\rho_b^2\rangle \times 10^{-18}$ (cm ⁻⁴)	T (°C)	a_c (Å)	$K\langle\rho_b^2\rangle \times 10^{-18}$ (cm ⁻⁴)
160	135 ± 7	5.2 ± 0.6	210	497 ± 110	0.46 ± 0.18
175	273 ± 58	1.1 ± 0.4	230	347 ± 82	0.67 ± 0.26
190	254 ± 17	1.3 ± 0.2			

Increasing the temperature up to 230 °C also led to an increase in the correlation length and a decrease in the scattered intensity. Measurements were in this case performed on the diffractometer LOQ, and longer counting times (~ 3 h) were used relative to experiments on D11. The results from least-squares fits are reported in Table III.

As previously mentioned, the scattered intensity in the pure copolymers is higher in the fully deuterated LCP than for the partially labeled and unlabeled LCPs. The relative intensity scaled approximately with the scattering length densities of the pure LCPs, which suggests that the scattering was related to the presence of microvoids in the material. However, the trend observed between results at different annealing temperatures and as a function of annealing time indicates that the scattering signal may be related to the structure of the system under study. In particular, the temperature and time dependences were consistent with optical microscopy measurements of LCPs. Coarsening of the schieleren texture was observed for isothermal annealing and temperature changes.²⁷ This was a consequence of growth in the domain size due to the disappearance of defects, i.e., disclinations. The observed signal may be related to a polydomain structure typical of liquid crystalline systems. Although the domains, constituted by regions of high local orientation, are too large to give rise to the observed signal (10^4 – 10^5 Å), the presence of a boundary region between domains may be responsible for the coherent signal. The measured correlation length represents the mean chord traversing the two phases of different scattering length density: the domains and a characteristic boundary zone between them. That is, the isotropic signal may originate with the structure of the disclinations.

Our results differ from previous studies on side-chain^{14–17} and main-chain^{18,19} LCPs, where the existence of signals superimposed on the single-chain scattering was not reported. However, similar Zimm plots were reported by Olbrich et al.²⁸ in their study of a copolyester of poly(ethylene terephthalate) (PET) and poly(*p*-hydroxybenzoic acid) (PHB). They found that a polymer containing a 60 mol % of PET that formed a liquid crystalline phase exhibited SANS patterns which gave nonlinear Zimm plots at low Q . The scattering patterns showed a Q^{-4} dependence at low Q that was attributed to particle scattering and related to undissolved PHB clusters. Copolyesters containing different concentrations of PET (e.g., 80 and 70%) gave linear Zimm plots. The later copolymers did not show liquid crystalline behavior.

A two-phase structure was also observed by Hashimoto et al.²⁷ for a LCP copolyester containing 60 mol % of PHB and 40 mol % of PET. Small-angle X-ray scattering (SAXS) measurements of the LC phase gave a correlation length of about 300 Å, which was attributed to segregation between the two different chemical units. A similar conclusion, that segregation between flexible and rigid units could be responsible for the isotropic scattering in the pure polymers, seems plausible, but the scattering intensity should be higher for the partially deuterated LCP than for the fully deuterated LCP, which is opposite

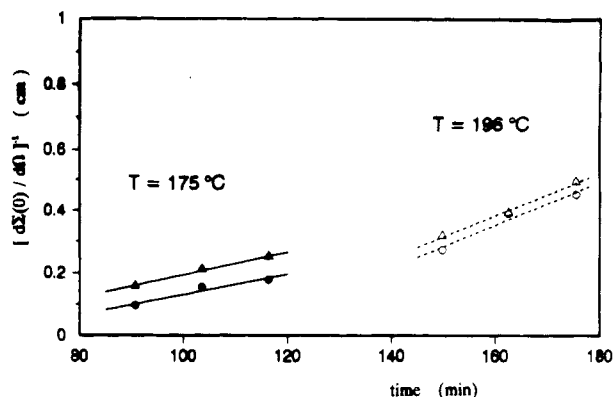


Figure 4. Values of intercept intensity at $Q = 0$ derived from fitting of Zimm plots, as a function of time for $T = 175$ (●,▲) and 196 °C (○,△). (●,○) From fitting of the component parallel to the field. (▲,△) From fitting of the perpendicular component.

to what was actually observed. Therefore, our observation of an isotropic SANS signal for pure polymers cannot be due to contrast between flexible and rigid units.

The coexistence of isotropic and nematic phases is another possible explanation for the scattering of the pure polymers. This possibility has been eliminated by NMR measurements that show no evidence of a biphasic up to 230 °C. A biphasic was observed by NMR between 230 and 250 °C. These results will be more fully described in another paper.

The Porod model, extended to account for the presence of a finite interphase,²⁹ offered an alternative method for the analysis of the scattering from the pure deuterated LCP. Both a cylindrical and a lamellar domain morphology seemed to describe the scattering patterns. The interphase thickness, t , calculated from the slopes of $\ln(Q^3 \times I(Q))$ versus Q^2 , for cylindrical domains, and $\ln(Q^2 \times I(Q))$ versus Q^2 , for lamellar domains, gave $t = 114 \pm 7$ and $t = 156 \pm 7$ Å, respectively.

Measurements of the Radius of Gyration. The scattering from mixtures of labeled and unlabeled LCP is characterized by two regions of different scattering behavior. At $Q > 0.015$ Å⁻¹, the single-chain scattering predominates, as illustrated by the linearity of $(d\Sigma/d\Omega)^{-1}$ versus Q^2 plots (Zimm plots) (Figure 2). At lower Q ($Q < 0.015$ Å⁻¹) deviations occur due to the presence of the extra scattering discussed above; at low Q , the square root of the scattered intensity has a Q^{-2} dependence. Due to the temperature and time dependences of the extra scattering, knowing the proper way to correct the scattering data for these effects was not obvious. However, because the signal due to the phase structure decreased very rapidly with Q , it seemed reasonable that it could be neglected in the single-chain scattering region, i.e., $Q > 0.016$ Å⁻¹.

The time dependence of the scattering from a 45% fully deuterated LCP mixture (45D6-H16) was investigated at two different temperatures: 175 and 196 °C. Data were fitted in the higher Q region according to eq 3 to derive the weight-average molecular weight and the projections of the radius of gyration, $R_{||}$ and R_{\perp} . The inverse of the extrapolated intensity at $Q = 0$ is plotted versus time in Figure 4 for a sample first annealed at 160 °C and then at 175 and 196 °C (the time dependence was not studied at 160 °C). The scattered intensity decreases with time, the decrease at 196 °C being faster than at the lower temperature. The time-dependent decrease in intensity corresponds to a decrease in M_w . As illustrated in Figure 5, the z -average radii of gyration, $R_{||}$ and R_{\perp} , also decrease with annealing time.

The decreasing M_w observed by SANS is due to the occurrence of transesterification reactions. Interchange

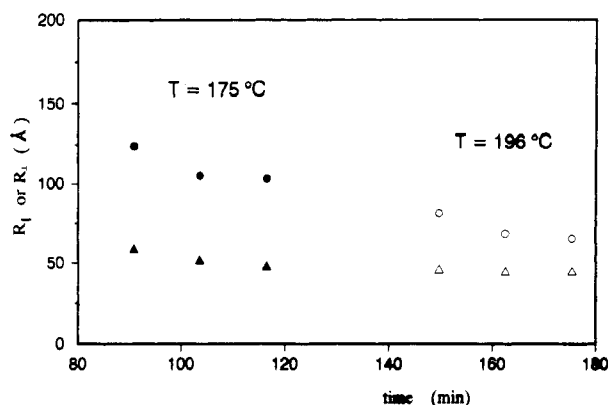


Figure 5. Components parallel (●,○) and perpendicular (▲,△) of the radius of gyration, $\langle R^2 \rangle_z^{1/2}$, as a function of time for $T = 175$ (●,▲) and 196 °C (○,△).

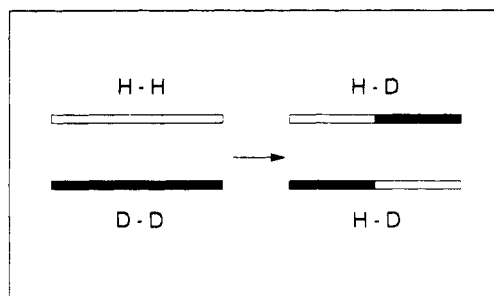


Figure 6. Schematic representation of a transesterification reaction (D, deuterated blocks; H, hydrogenous blocks).

reactions in polyesters above the melting temperature have been recently studied by SANS for poly(ethylene terephthalate) and PET-containing copolyesters.^{28,30-34} This technique has proven to be very useful in understanding the kinetics of transesterification.^{32,34}

As illustrated schematically in Figure 6, the result of transesterification is that polymer chains consisting of deuterated and hydrogenous blocks are formed from the initial mixture of hydrogenous and deuterated chains. The average degree of polymerization of the blocks and their radii of gyration are determined by the neutron scattering profiles. The chain-average molecular weight of the polymer is unchanged³⁰ by transesterification; the major effect is to produce the most probable distribution of molecular weight. For mixtures of hydrogenous and deuterated chains, the molecular weights and radii of gyration of the blocks determined by SANS will decrease as the reaction proceeds.

GPC (gel permeation chromatography) measurements carried out on a sample before and after SANS experiments were consistent with the SANS results. The initial M_w measured by GPC for the polymer mixture (50D2-H11) was $24\,000$ (corresponding to a light scattering value of $10\,600$). After more than 24 h of annealing at different temperatures, including the isotropic phase ($T > 250$ °C), the GPC M_w was reduced to $16\,000$ (corresponding to a light scattering value of 8810). During the same length of time the M_w determined by SANS decreased to 2000 . These results indicate that although partial decomposition did occur, as might be expected for prolonged annealing at high temperature, the extent of decomposition was not sufficient to explain the low M_w determined by SANS.

The kinetics of transesterification of poly(ethylene terephthalate)³² and a similar main-chain aromatic polyester³⁴ have been studied by SANS at much higher temperature. Even though our study was not focused on the kinetics of the reaction, it is interesting to compare

our results with data in the literature. To do this, we need to consider the effect of the activation energy, E_a . This was reported to be equal to 152 and 157 kJ mol⁻¹ in refs 32 and 34, respectively. The rate constants at 175 and 196 °C calculated from these values appear to be much lower than those experimentally determined in our work. The rate constant per mole of monomer units calculated from the data reported in the literature³⁴ is 8.51×10^{-7} s⁻¹, whereas the value estimated experimentally in our work was 0.0429 s⁻¹ at $T = 175$ °C. The discrepancy between the results could confirm the conclusions of Richards et al.³⁴ that the reaction proceeds via an active chain end mechanism. These authors studied the kinetics of the reaction using two polymers with M_w equal to 104 000 and 71 400, respectively. They found that the kinetics was faster by almost an order of magnitude for the lower molecular weight polymer. This appears to be consistent with our results, considering the very low M_w of the polymer used in this work.

Although values of $R_{||}$ and R_{\perp} depend on the extent of the reaction (since they indicate the average projections of R_z of the blocks), the ratio $R_{||}/R_{\perp}$ depends only on the polymer conformation. The ratio $R_{||}/R_{\perp}$ decreased from 2.1 ± 0.6 at 175 °C to 1.5 ± 0.3 at 196 °C, which indicates that the chain anisotropy decreased with increasing temperature in the nematic range as predicted by Warner et al. theory.^{8,12} Similar results were obtained from SANS measurements performed on mixtures of partially deuterated (D2) and nondeuterated (H16) polymer (30D2-H16). The chain anisotropy at 196 °C was comparable to the value calculated for 45D6-H16 ($R_{||}/R_{\perp} = 1.6 \pm 0.4$).

A low degree of anisotropy was observed at the low temperature (160 °C). This is probably related to insufficient alignment of the domain directors in magnetic fields at 160 °C. NMR measurements carried out on the labeled LCP (D2 and D6) indicated that a high extent of alignment can only be achieved for temperatures higher than 160 °C.

Higher degrees of chain extension were measured by D'Allest^{18,19} on a semiflexible liquid crystalline polymer containing *p*-azoxyanisole as the mesogenic unit. Measured R_z indicated that the polymer containing an even number of methylene units in the flexible spacer ($n = 10$) adopts an almost rodlike structure in the nematic phase and a random-coil conformation in the isotropic phase. No changes in chain conformation were detected in the pure nematic phase. This could be attributed to the low degrees of polymerization of the samples used for SANS, which is also consistent with the Warner et al. theory.

An attempt to distinguish between the two effects, transesterification and changes in chain conformation, which led to a decrease of the measured radius of gyration was made by considering the global z -average R_g (the corresponding isotropic value):

$$\langle R^2 \rangle_z = \langle R_x^2 \rangle_z + \langle R_y^2 \rangle_z + \langle R_z^2 \rangle_z \quad (6)$$

This should be less affected by any conformational change than $R_{||}$ since the projection of R_g in the perpendicular direction, R_{\perp} , is predicted to be independent of temperature in the mesophase range.^{8,12}

At first a procedure similar to the one adopted by Olbrich et al.²⁸ and Richards et al.³⁵ in treating the scattering from a main-chain liquid crystalline polyester was considered. The weight-average radius of gyration, $\langle R^2 \rangle_w^{1/2}$, was derived from the z -average (eq 6) by means of the relation³⁶

$$\langle R^2 \rangle_w = \langle R^2 \rangle_z \frac{1+u}{1+2u} \quad (7)$$

which applies to unperturbed Gaussian coils. The pa-

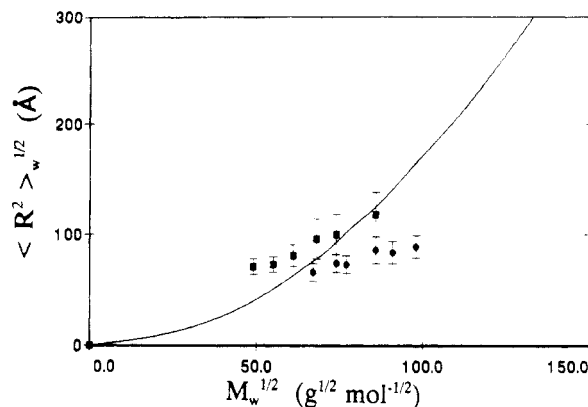


Figure 7. Molecular weight dependence of $\langle R^2 \rangle_w^{1/2}$ for 45D6-H16 (■) and 30D2-H16 (●) and comparison with a rodlike structure (—).

rameter u in eq 7 is related to the polymer polydispersity, $u = M_w/M_n - 1$, M_n being the number-average molecular weight. The polymer polydispersity, M_w/M_n , was assumed to be 2.5 ($u = 1.5$), which corresponds to the average GPC value for the as-made polymer.²¹ Transesterification should in principle lower this value to 2.0, but, in fact, the polydispersity of a sample annealed at high temperature for 24 h was measured by GPC to be $M_w/M_n = 2.6$. It should be added that these values of polydispersity refer to the entire polymer chains and not to the blocks. However, several authors have considered an identical M_w/M_n for the polymer chains and the blocks, in agreement with our assumption.^{32,35} It was pointed out that this is equivalent to assuming that the chemical attack is independent of the position along the chain.³²

The weight-average radius of gyration, $\langle R^2 \rangle_w^{1/2}$, evaluated from eq 7 is plotted in Figure 7 against the square root of the block M_w determined from the intercept at $Q = 0$ (eq 4) for 45D6-H16 and a sample (30D2-H16) containing 29% of partially labeled LCP (D2) and 71% of hydrogenous LCP (H16). The corresponding curve for a rod of zero cross section is also plotted in Figure 7 for comparison. That was calculated from

$$\langle R^2 \rangle_w = M_w^2 / 12M_L^2 \quad (8)$$

where M_L is the mass per unit length estimated from the length of the repeat unit in the fully trans conformation and the monomer molecular weight. At low M_w , the experimental data relative to 45D6-H16 appear to lie above the line drawn for a rodlike structure (Figure 7). This suggests that the random-coil model, implicitly applied by using eq 7, is probably not suitable for the description of our results. We then considered alternative models which may better represent the experimental data.

The z -average radius of gyration, $\langle R^2 \rangle_z^{1/2}$, calculated from eq 6 is plotted in Figure 8 versus the block M_w for 45D6-H16, 30D2-H16, and a sample containing 25% D2 and 75% hydrogenous LCP (H11). Comparison with the corresponding z -average radius of gyration³⁷

$$\langle R^2 \rangle_z = \frac{(1+3u)(1+2u)}{(1+u)^2} \frac{M_w^2}{12M_L^2} \quad (9)$$

for a rod (Figure 8) leads now to more consistent results. The radius of gyration approaches the rod values with decreasing block molecular weight. This is not unexpected in that, as predicted by the Warner theory, chains, or in this case blocks, composed of only 5–6 repeat units should become nearly fully extended in strong nematic field.

As illustrated in Figure 8 the molecular conformation appears to be rather extended although less than for a

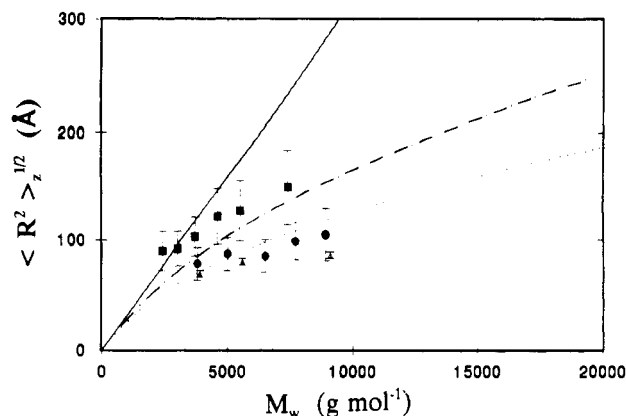


Figure 8. Blocks' z-average R_g plotted versus blocks' M_w for 45D6-H16 (■), 30D2-H16 (●), and 20D2-H16 (Δ) and comparison with $\langle R^2 \rangle_z^{1/2}$ calculated for a rodlike structure (—) and a wormlike chain with $l_p = 120$ Å (---) and $l_p = 60$ Å (···).

rodlike configuration. This type of behavior has been modeled in terms of wormlike chains. The wormlike chain model describes the conformation of a chain which approaches a Gaussian coil for high molecular weights and reduces to the rod limit for low M_w .³⁸ The z-average radius of gyration for a wormlike chain with persistence of direction and no persistence of curvature is given by the following expression:³⁷

$$\langle R^2 \rangle_z = \frac{1+2u}{1+u} \frac{L_{\text{cont}} l_s}{6} \left[1 - \frac{1+u}{1+2u} \frac{3l_s}{2L_{\text{cont}}} \left(1 - \frac{l_s}{L_{\text{cont}}} \right) - \frac{(1+u)^2}{1+2u} \frac{3l_s^3}{4L_{\text{cont}}^3} \left(1 - \left(1 + \frac{u}{1+u} \frac{2L_{\text{cont}}}{l_s} \right)^{-1/u} \right) \right] \quad (10)$$

The curve calculated from the above equation using a statistical length (l_s) of 240 ± 20 Å, which is equivalent to a persistence length (l_p) of 120 Å, and $u = 1.5$ is shown in Figure 8. Such a value of the persistence length which corresponds to 4.5–5 times the length of the repeat unit (calculated for a fully trans conformation, 27.4 Å; determined by WAXD, 24 Å) appears consistent with the dependence of the block $\langle R^2 \rangle_z^{1/2}$ on the block M_w shown in Figure 8. That is, the average conformation of the blocks becomes highly extended when its length approaches the persistence length.

The z-average radius of gyration $\langle R^2 \rangle_z^{1/2}$ for mixtures of partially deuterated (D2) and hydrogenous (H16 or H11) polymers is also plotted as a function of the block M_w in Figure 8. Samples containing the partially labeled LCP give lower R_z than 45D6-H16. In this case, the persistence length estimated from the M_w dependence is only 58 Å, approximately half the value calculated for 45D6-H16.

This discrepancy and its possible explanation will now be discussed in some detail. Radii of gyration, plotted in Figure 8, were calculated from eq 6 for 30D2-H16. Experiments on the 25% partially deuterated blend (20D2-H11) were performed in the absence of a magnetic field, and the z-average R_g was directly computed from Zimm plots according to the procedure for isotropic scattering. Figure 8 shows good agreement between the data from 30D2-H16 and 20D2-H11. The discrepancy between results from different polymer mixtures is not due entirely to the assumptions inherent to the method for calculating $\langle R^2 \rangle_z^{1/2}$ (eq 6).

The molecular weights of the labeled and unlabeled polymers are listed in Table I. There was a large difference between M_w of the partially and fully deuterated polymers, D2 and D6, respectively. For only 45D6-H16 were the M_w of the labeled and unlabeled LCP closely matched as

is desirable in the SANS analysis. The effect of differences in M_w in a mixture containing labeled and unlabeled chains has been investigated by Boué et al.³⁹ Expressions for correcting experimental values of M_w and R_z have been derived^{39,40} and were used to calculate correction factors for the 30D2-H16 and 20D2-H11 data. Since the molecular weight of the unlabeled polymer was higher than that for the labeled LCP, the corrected M_w and R_z were lower than the experimentally determined values. This makes the difference between the results for the 45D6-H16 mixture and D2-H16 or H11 even larger.

Disagreement between statistical or persistence lengths from the fully and partially deuterated polymer mixtures may be related to the difference between the deuterated parts in the two polymer chains. If the polymer chain is regarded as a copolymer composed of rigid units (R) and flexible spacers (F), three structure factors need to be considered:^{13,41}

$$\frac{d\Sigma(Q)}{d\Omega} = K_R^2 S_R(Q) + K_F^2 S_F(Q) + 2K_R K_F S_{RF}(Q) \quad (11)$$

$S_R(Q)$ is for the rigid part, $S_F(Q)$ for the flexible spacer, and $S_{RF}(Q)$ for the cross term. K_R and K_F are the contrasts calculated for the different units in the deuterated-hydrogenous polymer mixture. K_R^2 , K_F^2 , and $2K_R K_F$ determine the relative influence of S_R , S_F , and S_{RF} on the measured structure factor. If one considers the neutron contrasts for the rigid and flexible units, it appears that the mixture containing the partially deuterated LCP, $C_{27}H_{14}D_{18}N_2O_4$, could give rise to a higher contribution from the flexible part, whereas, in the fully deuterated mixture, all contributions would be important.

The structure factors S_R , S_F , and S_{RF} are related to the radii of gyration R_R^2 and R_F^2 and the cross term L^2 . The radius of gyration for a copolymer constituted of units R and F is given by⁴¹

$$(R_g)_{\text{app}}^2 = yR_R^2 + (1-y)R_F^2 + y(1-y)L^2 \quad (12)$$

L^2 being the mean-square distance between the centers of mass of the R and F units. Considering y as a mean contrast between the two units, one can estimate the coefficients in eq 12

$$(R_g)_{\text{app}}^2 = 0.259R_R^2 + 0.741R_F^2 + 0.192L^2 \quad (13)$$

for the partially deuterated polymer mixture and

$$(R_g)_{\text{app}}^2 = 0.583R_R^2 + 0.417R_F^2 + 0.243L^2 \quad (14)$$

for the fully deuterated copolymer. Equations 13 and 14 may possibly account for the disagreement between $(R_g)_{\text{app}}^2$ from the polymer mixture 45D6-H16 and the two mixtures 30D2-H16 and 20D2-H11. Measurements on a mixture of hydrogenous and deuterated LCP, labeled in the rigid aromatic part only, may be able to confirm this.

Conclusions

A main-chain semiflexible liquid crystalline polyester was studied by SANS. Data analysis shows the existence of a two-phase structure for pure samples (fully and partially deuterated as well as unlabeled) within the nematic phase range. The isotropic signal was found to be temperature and time dependent. The calculated correlation length increases with annealing time and with increasing temperature.

The temperature and time dependences of the scattering signal seem consistent with a domain structure with boundary regions of different scattering length densities, between the domains. The density profile in the inter-

domain regions could not be simply modeled by a uniform density, as suggested by a Porod analysis performed on the same samples. One hypothesis, though as yet unconfirmed, is that the disclination structure gives rise to an isotropic signal.

SANS experiments performed on a mixture of labeled (D6) and unlabeled (H16) polymers, aligned in a magnetic field in the nematic phase range, revealed the occurrence of transesterification. The measured M_w and the radius of gyration (as well as its projections) decreased as a function of time and temperature.

SANS measurements suggested that stiffening of the polymer chain occurred in the nematic phase. A persistence length of approximately 120 ± 10 Å was estimated from the molecular weight dependence of the radius of gyration in the temperature range between 175 and 196 °C using a wormlike chain model. This corresponds to approximately 5 times the length of a repeating unit, which is considerably higher than the persistence length of 24 Å, or one monomer unit, that was measured in solution for the same polymer.²¹ The value of persistence length in the fully deuterated-hydrogenous LCP mixture was considered to be more reliable than the correspondent value in the partially deuterated-hydrogenous LCP sample.

Lower values of the persistence length were reported by Richards et al.³⁵ for a main-chain LCP prepared from hydroxybenzoic acid, hydroquinone, and isophthalic acid. In that study, measurements performed below T_m indicated stiffening of the polymer molecules with increasing temperature and the persistence length varied from 9 Å at 175 °C to 44 Å at 250 °C (near the solid to nematic transition). Presumably higher values of the persistence length could be measured within the nematic phase.

Our results appear to be in disagreement with SANS data reported for copolyesters of poly(ethylene terephthalate) (PET) and poly(*p*-hydroxybenzoic acid) (PHB).²⁸ Polymers with a PET content from 80 to 60 mol % were studied. The copolyester containing 60 mol % of PET exhibited LC behavior. The statistical length was calculated from SANS data as a function of the content in PHB stiff units. The liquid crystalline polyester showed an increase in the statistical length which could be explained in terms of an increase in the PHB content but no further increase due to conformational changes in the nematic phase. The authors concluded that in the nematic phase the chains had values of the radius of gyration corresponding to unperturbed coils. It is probably worth adding that the results on PET/PHB copolyesters are in contradiction not only to our data but also to the observation made by Richards et al.³⁵ and D'Allest et al.^{18,19} that conformational changes occur at the transition to the nematic phase.

Due to transesterification, only the ratio $R_{||}/R_{\perp}$ is indicative of changes in chain conformation. Changes in chain extensions were observed by SANS measurements on samples aligned in the nematic phase. The ratios $R_{||}/R_{\perp}$ decreased from 2.1 to 1.5 with increasing temperature between 175 and 196 °C. This seems to at least qualitatively confirm the theoretical predictions of Warner et al.^{8,12}

The results of this study differed from previous measurements on a main-chain semiflexible LCP,^{18,19} which may have been a consequence of the low degree of polymerization of the samples used. D'Allest et al. observed a large change in the chain dimensions at the nematic to isotropic transition in samples aligned in a magnetic field. The radii of gyration in the nematic phase

approached the fully extended conformation.

The occurrence of transesterification prevented a detailed study of chain conformation in the entire mesophase range (due to the fast kinetics of the reaction compared with the required SANS counting times). For long annealing times, only an equilibrium value of M_w and R_g was measured. The molecular weight of the deuterated blocks corresponded to 5–6 monomer units. The measured R_g indicated a fully extended conformation, as expected for low degrees of polymerization of the deuterated blocks.

There still remains a number of open questions regarding the polymer conformation in liquid crystalline phases, as indicated by apparent discrepancies between the published data. Probably one of the major reasons for this is that in these studies experiments were conducted on polyesters. SANS measurements on polymers of the noncondensation type will certainly contribute in the future to the clarification of the conformational behavior of LCPs.

Acknowledgment. V.A. thanks Montedison S.p.A. for financial support. V.A. and J.S.H. thank the Science and Engineering Research Council for support during the experiments at ILL and RAL. R.A.W. and A.L.C. thank the donors of the Petroleum Research Fund, administered by the American Chemical Society, for partial support of the research. We all thank Dr. A. Rennie, Dr. P. Terech, and Dr. S. M. King for technical assistance during SANS experiments. We also thank Dr. R. Richards, Dr. M. Warner, and Dr. P. Sixou and his research group for helpful discussions.

References and Notes

- (1) Toyne, K. J. In *Thermotropic Liquid Crystals*; Gray, G. W., Ed.; John Wiley & Sons: New York, 1987; p 28.
- (2) *Polymer Liquid Crystals*; Ciferri, A., Krigbaum, W. R., Meyer, R. B., Eds.; Academic Press: New York, 1982.
- (3) Roviello, A.; Sirigu, A. *J. Polym. Sci., Polym. Lett. Ed.* **1975**, *13*, 455.
- (4) Ober, Ch. K.; Jin, J.; Lenz, R. W. *Adv. Polym. Sci.* **1984**, *59*, 103.
- (5) *High Modulus Polymers*; Zachariades, A. E., Porter, R. S., Eds.; Marcel Dekker: New York, 1988.
- (6) Onsager, L. A. *Ann. N.Y. Acad. Sci.* **1949**, *51*, 627.
- (7) Flory, P. J. *Adv. Polym. Sci.* **1984**, *59*, 1.
- (8) Warner, M.; Gunn, J. M. F.; Baumgartner, A. B. *J. Phys.* **1985**, *A18*, 3007.
- (9) ten Bosch, A.; Maissa, P.; Sixou, P. *Phys. Lett.* **1983**, *A94*, 298.
- (10) ten Bosch, A.; Maissa, P.; Sixou, P. *J. Chem. Phys.* **1983**, *79*, 3462.
- (11) de Gennes, P.-G. In *Polymer Liquid Crystals*; Ciferri, A., Krigbaum, W. R., Meyer, R. B., Eds.; Academic Press: New York, 1982; p 124.
- (12) Wang, X. J.; Warner, M. *J. Phys.* **1986**, *A19*, 2215.
- (13) Higgins, J. S.; Maconnachie, A. In *Methods of Experimental Physics*; Academic Press: New York, 1987; Vol. 23, p 287.
- (14) Kirste, R. G.; Ohm, H. G. *Makromol. Chem., Rapid Commun.* **1985**, *6*, 179.
- (15) Keller, P.; Carvalho, B.; Cotton, J. P.; Lambert, M.; Moussa, F.; Pepy, G. *J. Phys. Lett.* **1985**, *46*, L-1065.
- (16) Moussa, F.; Cotton, J. P.; Hardouin, F.; Keller, P.; Lambert, M.; Pepy, G.; Mauzac, M.; Richard, H. *J. Phys. (Paris)* **1987**, *48*, 1079.
- (17) Ohm, H. G.; Kirste, R. G.; Oberthür, R. C. *Makromol. Chem.* **1988**, *189*, 1387.
- (18) D'Allest, J. F.; Sixou, P.; Blumstein, A.; Blumstein, R. B.; Texeira, J.; Noirez, L. *Mol. Cryst. Liq. Cryst.* **1988**, *155*, 581.
- (19) D'Allest, J. F.; Maissa, P.; ten Bosch, A.; Sixou, P.; Blumstein, A.; Blumstein, R. B.; Texeira, J.; Noirez, L. *Phys. Rev. Lett.* **1988**, *61*, 2562.
- (20) Iannelli, P.; Roviello, A.; Sirigu, A. *Eur. Polym. J.* **1982**, *18*, 745.
- (21) Roviello, A.; Sirigu, A. *Eur. Polym. J.* **1979**, *15*, 61.
- (22) Cimecioglu, A. L.; Fruitwala, H.; Weiss, R. A. *Makromol. Chem.* **1990**, *191*, 2329.
- (23) *Neutron Research Facilities at the Institute Laue-Langevin High Flux Reactor*; ILL: Grenoble, France, 1986.
- (24) *ISIS User Guide-Experimental Facilities at ISIS*, RAL-88-030, Rutherford Appleton Laboratory, 1988.

- (24) Ghosh, R. E. *A Computing Guide for Small Angle Scattering Experiments*; ILL Report No. 84BE05T, Institute Laue-Langevin, Grenoble, France, 1989.
- (25) Cotton, J. P.; Decker, D.; Benoit, H.; Farnoux, B.; Higgins, J.; Jannink, G.; Ober, R.; Picot, C.; des Cloizeaux, J. *Macromolecules* **1974**, *7*, 863.
- (26) Debye, P.; Bueche, M. A. *J. Appl. Phys.* **1949**, *20*, 518. Debye, P.; Anderson, H. R.; Brumberger, H. *J. Appl. Phys.* **1957**, *28*, 679.
- (27) Shiwaku, T.; Nakai, A.; Hasegawa, H.; Hashimoto, T. *Macromolecules* **1990**, *23*, 1590.
- (28) Olbrich, E.; Chen, D.; Zachmann, H. G.; Lidner, P. *Macromolecules* **1991**, *24*, 4364.
- (29) Richards, R. W.; Thomason, J. L. *Polymer* **1983**, *24*, 1089.
- (30) Gilmer, J. W.; Wiswe, D.; Zachmann, H. G.; Kugler, J.; Fischer, E. W. *Polymer* **1986**, *27*, 1391.
- (31) Wu, W.; Wiswe, D.; Zachmann, H. G.; Hahn, K. *Polymer* **1985**, *26*, 655.
- (32) Kugler, J.; Gilmer, J. W.; Wiswe, D.; Zachmann, H. G.; Hahn, K.; Fischer, E. W. *Macromolecules* **1987**, *20*, 1116.
- (33) McAlea, K. P.; Schultz, J. M.; Gardner, K. H.; Wignall, G. D. *Polymer* **1986**, *27*, 1581.
- (34) MacDonald, W. A.; McLenaghan, A. D. W.; McLean, G.; Richards, R. W.; King, S. M. *Macromolecules* **1991**, *24*, 6164.
- (35) MacDonald, W. A.; McLenaghan, A. D. W.; McLean, G.; Richards, R. W.; King, S. M. *Macromolecules* **1992**, *25*, 826.
- (36) Greschner, G. S. *Makromol. Chem.* **1973**, *168*, 273.
- (37) Oberthür, R. C. *Makromol. Chem.* **1978**, *179*, 2693.
- (38) Benoit, H.; Doty, P. *J. Phys. Chem.* **1953**, *57*, 958.
- (39) Boué, F.; Nierlich, M.; Leibler, L. *Polymer* **1982**, *23*, 29.
- (40) Crist, B.; Graessley, W. W.; Wignall, G. D. *Polymer* **1982**, *23*, 1561.
- (41) Cotton, J. P.; Benoit, H. *J. Phys.* **1975**, *36*, 905.

Registry No. DMB/decanedioic acid/dodecanedioic acid, 84234-13-9.